Shear-Rate Dependent Surface Tension of Glass-Forming Fluids

Linnea Heitmeier and Thomas Voigtmann*

Institute of Frontier Materials on Earth and in Space, Deutsches Zentrum für Luft- und Raumfahrt (DLR), 51170 Köln, Germany and Department of Physics, Heinrich-Heine Universität Düsseldorf, Universitätsstraße 1, 40225, Düsseldorf, Germany

(Received 8 August 2025; accepted 21 January 2026; published 11 February 2026)

We investigate the interface of a glass-forming fluid showing non-Newtonian rheology. By applying shear flow in the interface, we observe that the surface tension depends on the shear rate. Importantly, the standard way of determining surface tension from the pressure anisotropy caused by the interface can give rise to an effective surface tension in the non-Newtonian fluid that mixes bulk and interface properties. We show how the pressure anisotropy can be used to clearly define the bulk and interface regions and extract a genuine shear-rate dependent surface tension. The results have implications for measurement techniques related to the interfacial rheology of complex fluids.

DOI: 10.1103/wqzf-kk36

The surface of glass-forming fluids is home to many intriguing dynamical phenomena. Glasses are covered by layers of enhanced molecular mobility [1,2], providing an amorphous analog to surface melting, the physical mechanism conjectured to facilitate ice skating at low temperatures. The high mobility near the surface enables the layerwise fabrication of ultrastable glasses with unique mechanical properties [3–5], and strongly influences the properties of polymer films [6]. The surface induces a dynamical penetration depth into the bulk that changes nonmonotonically with temperature and allows to disentangle the change in mechanisms of relaxation close to a dynamical crossover temperature T_c [7].

Surface tension is a key parameter characterizing interfaces of complex fluids [8], but not many theoretical studies address it in the dynamical crossover regime close to the kinetic arrest transition. This is despite the significance in applications for films and coatings, in interfacial rheology in general [9], for certain 3D-printing techniques [10], and also for theoretical concerns. The surface tension of amorphous structures in contact with each other is posited by some theories to play a key role in the dynamical crossover from supercooled liquid to glass [11,12].

Glass formers typically are shear-thinning and yield-stress fluids, i.e., close to T_c their viscosity strongly decreases with the flow rate, and they flow only above a certain threshold stress [13,14]. Reliable experimental data for the surface tension of such non-Newtonian fluids are rare, since the emerging yield stress impedes measurements [15,16]. Because of the associated slow relaxation timescale of the fluid, hysteresis effects can arise. For example, Jørgensen *et al.* [16] used a liquid-bridge tensionmeter and found the apparent surface tension of carbopol dispersions to be systematically higher in expansion than in compression. They rationalized this finding with an elastoplastic model of the fluid, and attributed it to the existence of a yield stress.

This poses a number of questions: first, how does the surface tension, a parameter that is typically evaluated from "static" pressure differences across an interface, couple to the non-Newtonian rheology of highly viscoelastic fluids, a typical "dynamic" effect in the bulk? Second, since the bulk rheology of the shear-thinning fluid depends very sensitively on the shear rate, what is the effect of fluid flow on the (apparent) surface tension?.

We address these questions by molecular dynamics simulations of a prototypical model of a glass-forming fluid (involving no polymeric or suspension effects), in a simple setup involving a planar surface. Our simulations reveal how an apparent surface tension arises in non-Newtonian fluids that is a mixture of bulk rheology and genuine surface effects.

We consider the standard Kob-Andersen binary Lennard-Jones (LJ) mixture [17] at fixed number density $\rho = 1.2$ using the open-source package LAMMPS [18]. Units of length, σ, time, τ_0, and energy are all in standard LJ units related to the larger particles. The simulations start from bulk liquids in the NVT ensemble, which are equilibrated at $T_i = 2.0$ for at least $500\tau_0$, cooled to the target temperature T, and then equilibrated again for up to $10^6\tau_0$ (depending on T). We use $N = 5000$ ($N = 10\,000$) particles corresponding to a cubic box of size $L = L_x = L_y = 13\sigma$ and $L_z = 24.6\sigma$ (49.2σ) for the small (large) system. For the determination of the surface tension from capillary theory,

*Contact author: thomas.voigtmann@dlr.de

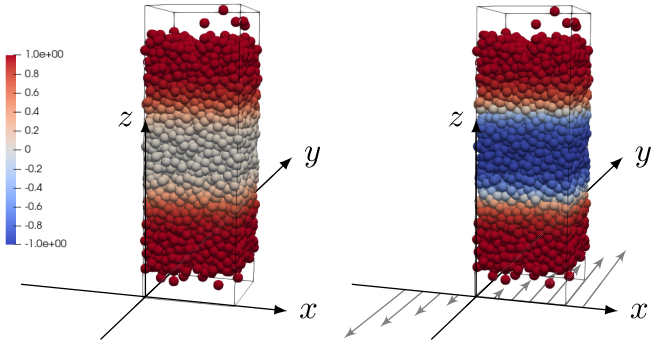

FIG. 1. Snapshots of the simulation setup without (left) and with (right) imposed shear. Only the central part of the box along z is shown for clarity. We impose "in-plane" shear, as shown by the arrows in the coordinate system. Particles are colored according to $\Delta p = p_z - (p_x + p_y)/2$ normalized to the interval $[-1, 1]$; see Fig. 3.

alongside the small system, a wide system with $L = 18\sigma$ with $N = 9564$ particles was used.

After equilibration, the simulation box was enlarged to $L_z = 160\sigma$, keeping the fluid in the center of the box where around $z = 0$, bulk properties are recovered [7]. The interfaces were then relaxed for $250\tau_0$ before measurements were performed. Shear flow with rate $\dot{\gamma}$ is imposed in the (x, y) plane tangential to the surface (see Fig. 1) using the SLLOD equations; this is also motivated by the tangential character of the surface tension [19–23]. Note that our shear protocol keeps the total surface area constant, which is conceptually important for viscoelastic fluids [23]. Surface tension values were averaged over at least $2000\tau_0$. Inspection of the z-dependent density profiles revealed no particle-species segregation.

We use two independent methods to determine the surface tension $\hat{\sigma}$: the first is by *ad hoc* extending the expression from equilibrium statistical physics [24] to our nonequilibrium setting, evaluating the pressure difference

$$\hat{\sigma} = \frac{1}{2}\int dz \left[p_z(z) - \frac{1}{2}(p_x(z) + p_y(z)) \right]. \tag{1}$$

In our simulation setup there are two interfaces that contribute equally (see also Fig. 3 below) to the integral, and thus a factor $1/2$ is included in Eq. (1). Some remarks are in order. The definition of a spatially resolved pressure tensor requires care, as discussed in detail in Ref. [25]. A crucial requirement is that the pressure $p_z(z)$ normal to the interface is constant as a function of z; this we have checked to be fulfilled in our calculations [26]. Equation (1) also assumes the integrand to vanish in the bulk regions. This is no longer the case for a non-Newtonian fluid under shear, where shear-dependent normal-pressure differences arise. We will discuss this in more detail below. The use of Eq. (1) outside equilibrium is not *a priori* justified.

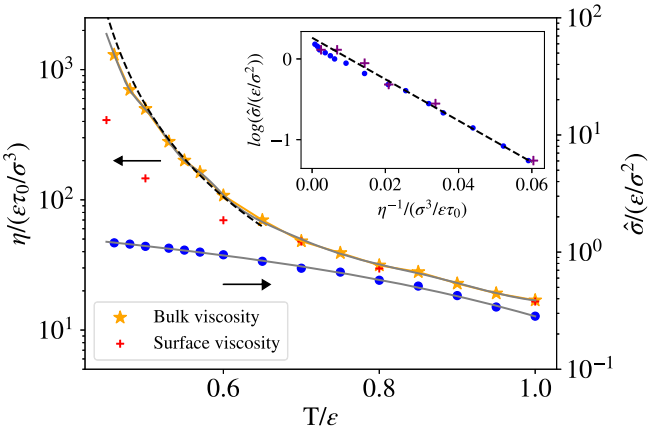

FIG. 2. Bulk viscosity (star symbols) and surface tension (circles) of the quiescent system as function of temperature. Solid lines are guides to the eye. A dashed line indicates the power law predicted by mode-coupling theory, and crosses indicate the surface-layer viscosity (see text). Inset: logarithm of the surface tension as a function of inverse viscosity (circles) and inverse surface-layer viscosity (crosses).

We thus also determine the surface tension via the width of the density profile Δ [27–29],

$$\Delta^2 = \Delta_0^2 + \frac{k_B T}{2\pi\hat{\sigma}} \ln(L/B_0), \tag{2a}$$

where we fit the density profile according to

$$\rho(z) = \frac{\rho_l}{2} - \frac{\rho_l}{2} \tanh\left(\frac{2(z - z_0)}{\Delta} \right), \tag{2b}$$

with the bulk liquid density ρ_l, and z_0 a fit parameter for the position of the interface. In Eq. (2), Δ_0 and B_0 are unknown prefactors determined from fits for two different L (small and wide system).

We checked that our results recover previously reported surface-tension values for the one-component quiescent LJ fluid [30,31]. For reference, the bulk viscosity was determined using the standard Green-Kubo relation [32] in simulations of the bulk fluid, using a correlation time of up to $100\tau_0$.

We begin by summarizing the temperature dependence in the quiescent system. As the glass transition is approached, the viscosity of the bulk fluid strongly increases for around 2 orders of magnitude in the interval $T = [0.5, 1]$ studied here (stars in Fig. 2). The data is in the regime of the mode-coupling theory (MCT) of the glass transition: close to the crossover temperature T_c of MCT, the viscosity shows power-law growth, $\eta \sim |T - T_c|^{-\gamma}$ from which deviations set in at lower temperatures (a dashed line in Fig. 2 indicates the power law with $T_c = 0.4$ and $\gamma = 2.35$).

In the same temperature interval, the surface tension (circles) increases by almost a factor of 4. An empirical

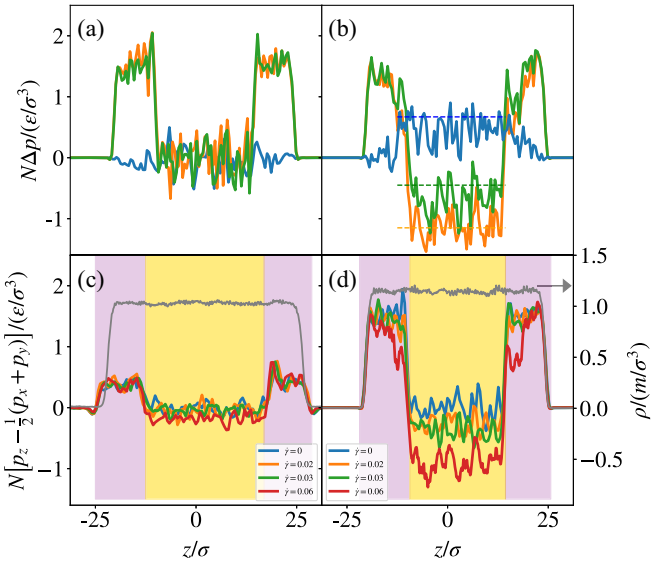

FIG. 3. Pressure differences across the interface. Top panels show $\Delta p_{\alpha\beta} = p_\alpha - p_\beta$ (blue, Δp_{xy}; green, Δp_{xz}; orange, Δp_{yz}) for temperature $T = 0.6$ in (a) the quiescent system and (b) with shear rate $\dot\gamma = 0.06$. Dashed lines in (b) correspond to normal stresses obtained from separate simulations of a bulk system. Bottom panels show the relevant pressure difference for the surface tension, $-(\Delta p_{xz} + \Delta p_{yz})/2$, for (c) temperature $T = 1$, and (d) $T = 0.6$. Color shadings indicate the z intervals identified as bulk and surface regions. All pressure values are multiplied by the number of particles in the respective z bin to mitigate fluctuations from normalization. In the bottom panels, gray lines (corresponding to right y axes) show the corresponding density profiles.

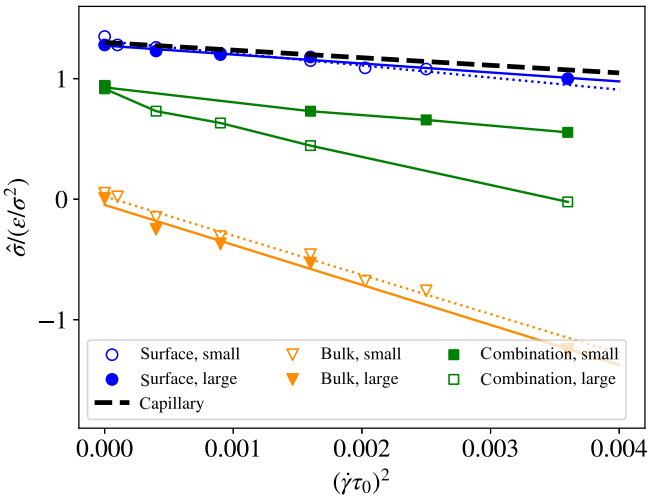

FIG. 4. Shear-rate dependence of the surface tension, as a function of the square shear rate $\dot\gamma^2$, for the Kob-Andersen mixture at $T = 0.6$. Blue symbols show values extracted from the pressure difference, a dashed line the trend extracted from capillary wave analysis. The contribution from the bulk of the non-Newtonian fluid (orange) leads to a system-size dependent effective surface tension (green), if evaluated by the pressure difference.

relation that links the surface tension and the viscosity has been proposed [33,34]: $\ln(\hat\sigma) = \ln(A) + B/\eta$ with fitting parameters A and B. We observe this to hold reasonably well (only) in the not-too-viscous regime ($\eta \lesssim 50$; inset of Fig. 2). For lower temperatures, we see deviations that we attribute to the slow structural relaxation affecting the viscosity: while the viscosity strongly grows, the surface tension appears to saturate (or grow less strongly) as the MCT transition is approached.

Particles close to the surface of a glass-forming fluid retain higher mobility than in the bulk [1,2,35]. It hence suggests itself to define a surface-layer viscosity that might bear a closer connection to the surface tension since it will grow less strongly than the bulk viscosity.

We have defined a surface-layer viscosity by constraining the Green-Kubo integral to particles starting in z layers close to the surface. The notion of "close" can be made precise by looking at the normal-stress differences, $\Delta p_{\alpha\beta} = p_\alpha - p_\beta$, where $\alpha, \beta \in \{x, y, z\}$. Recall that in the isotropic bulk, all $\Delta p_{\alpha\beta} = 0$. Close to the surface, the values for $\beta = z$, $\alpha \in \{x, y\}$, deviate from zero since the surface induces an anisotropy. This allows to clearly distinguish a surface layer [cf. Fig. 3(a)]. Note that this surface layer is significantly wider than the width of the density profile [Figs. 3(c) and (d)]. The surface-layer viscosity thus defined indeed follows the empirical relation to the surface tension more closely (crosses in Fig. 2), although approaching to T_c a decoupling still appears to occur (note that the lowest-T data point in our simulation deviates). We leave this question for a future study.

Now we turn to surfaces with in-plane shear flow. Glass formers are non-Newtonian fluids, featuring nonvanishing normal-stress differences in the bulk. In particular, the first normal-stress difference in the bulk in our setup is defined as $N_1 = \sigma_{yy} - \sigma_{xx} = \Delta p_{xy}$ [36] and is expected to be positive according to standard rheological models. This is observed in the center of the liquid slab [Fig. 3(b), around $z = 0$] and confirmed by separate bulk simulations.

Crucially, the surface-near region remains different: here, pressure differences are related to the surface tension, and separate from the bulk. The changes in these regions will be related to a change in surface tension under shear. They become more pronounced at lower temperatures, as T_c is approached, while at higher temperatures the effect vanishes (lower panels of Fig. 3). As shown by the density profiles (gray lines in Fig. 3) we do not observe systematic density changes in the system, and thus the surface-tension and viscosity effects that we discuss here are not related to a change in density.

However, the bulk values give nontrivial contributions to the surface-tension integral that are specific to non-Newtonian fluids, and need to be taken into account when determining the surface tension of the sheared fluid from

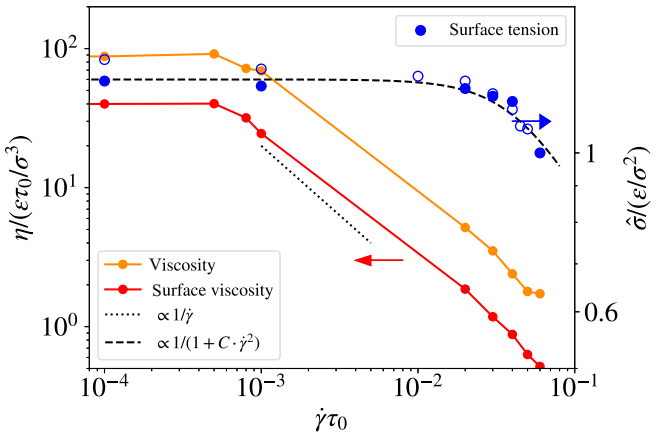

FIG. 5. Viscosity, surface-layer viscosity, and surface tension as functions of shear rate for $T = 0.6$. A dotted line indicates $1/\dot{\gamma}$, the shear-thinning asymptote expected on dimensional grounds. The dashed line is a fit to the surface tension values that crosses over from a constant to a $1/\dot{\gamma}^2$ behavior.

Eq. (1). If not disentangled, an apparent surface tension is obtained that shows a pronounced system-size effect (Fig. 4, green symbols). Larger systems are more strongly influenced by the non-Newtonian bulk rheology, to the point that the apparent surface tension might even vanish at large shear rates. It should be noted that this is not a destabilization of the interface; it is rather a nonequilibrium signature of the driven system, similar to what has been observed in active fluids [37,38].

It is thus crucial to separate the two regions in z—the surface layer identified by positive $\Delta p_{\alpha z}$, and the bulk liquid where these quantities have opposite sign (blue and orange symbols in Fig. 4). Both depend quadratically on the shear rate, as is expected from the symmetry of the problem under reversal of the flow direction.

Intuitively, it is the pressure drop across the surface layer that relates to the surface properties. We confirm this by determining the surface tension from an analysis of the density profile [Eq. (2)]. Since this procedure determines $\hat{\sigma}$ only up to a prefactor, we have adjusted this to match the value obtained from Eq. (1) at zero shear rate. The results for the $\dot{\gamma}$ dependence then are in very good agreement with each other (dashed black line in Fig. 4).

These results show that there is a genuine shear-rate dependence of the surface tension in the non-Newtonian fluid that can be distinguished from the bulk rheology, but is still coupled to it. [In the Newtonian fluid represented by $T = 1$, we do not observe a significant shear-rate effect, as shown by Fig. 3(c).] The change in surface tension is not just a consequence of a change in viscosity, as the empirical scaling relation discussed around Fig. 2 might have suggested. This is clearly seen by comparing the shear-rate dependencies (Fig. 5). By symmetry, the shear-thinning viscosity should decrease as $1/|\dot{\gamma}|$ [13]; a somewhat weaker decay is observed in the simulation, consistent with earlier results [39]. Also the surface-layer viscosity that we defined follows this trend (circle symbols in Fig. 5). The onset of shear thinning is at $\dot{\gamma}\tau_0 \ll 1$, indicating that it is the slow structural relaxation time ($\tau \gg \tau_0$) that sets the relevant timescale for shear thinning. The surface tension, properly disentangled from the bulk rheology, follows a $1/\dot{\gamma}^2$ "shear-thinning" law, but importantly with an onset at much higher $\dot{\gamma}\tau_0$ (and thus higher than expected for the bulk normal-stress differences [40]).

In summary, we have shown that the surface tension of a typical glass-forming viscoelastic fluid shows a strong shear-rate dependence. In non-Newtonian fluids, normal-stress differences in the bulk and surface anisotropy of the stress tensor contribute to an *effective surface tension* that is measured using standard techniques that are based on the pressure drop across a liquid film and mix two different contributions. One contribution is a genuine surface contribution, and it comes from the pressure anisotropy in the layers near the surface. In the simulation they can be clearly identified through the different sign of $\Delta p_{\alpha z}$ with respect to the bulk. In addition, there is a nontrivial bulk contribution arising from nonvanishing normal-stress differences, a typical non-Newtonian fluid effect.

This might explain why the determination of surface tension values from pressure balances of bulk viscoelastic samples is difficult, as in experiments it will be difficult to disentangle the pure surface from a bulk contribution. Also, hysteresis effects as previously reported might be arising from a non-Newtonian bulk contribution: we have monitored the transient evolution of the pressure differences after switching on the shear flow, and found no sign of slow relaxation in the surface contribution. But the bulk quantities are known to exhibit patterns of slow relaxation. Also, a changing volume-to-surface ratio, as in techniques where a fluid droplet is expanded or compresses, might see effects from different mixing of surface and bulk contributions.

Our findings should be relevant to various techniques measuring interfacial rheological properties in films of complex fluids [41–43] and even for the printability of bioinks in surface-tension assisted 3D-printing techniques [44]. For example, biofilms are known to exhibit complex rheology, and characterization of their mechanical surface properties is an important aspect in their growth and removal [45,46]. The complex interactions in such films can render the surface tension anisotropic [9], and our method of imposing in-plane shear flow in different directions might be a straightforward way to interrogate the characteristics of the interface in such cases.

We expect our results to be generic and applicable to a wide range of non-Newtonian fluids, including, e.g., polymer melts. So far we are not aware of systematic studies, although in the rheology of foams a flow-rate dependent surface tension has been discussed [47,48]. Also a recent study of soft silicone gels [49] found a change in surface tension as the material was deformed.

Understanding the link of liquid-state surface tension and emergent elastic contributions across the glass transition will be a future field of study that also might help to understand the nature of kinetic arrest further.

On a more theoretical note, it has been shown that the surface of glass-forming fluids reveals nonmonotonic changes in the dynamical correlation length governing glassy dynamics [1,7]. A crucial point there was to distinguish a static length scale linked to the density profile, from a much larger dynamic one linked to the structural-relaxation dynamics. To explore the link between this dynamic length scale and the depth of the surface layers inferred from the pressure anisotropy remains an interesting open question, as it links inherent features of glassy dynamics to surface properties, and thus might provide further insight into theories of dynamical heterogeneities. Also, we leave for further discussion the fate of the surface tension in the deeply supercooled regime (below the MCT transition): eventually, the viscoelastic nature of the glass-forming fluid will be felt, and as one approaches the soft solid state, surface tension and surface energies need to be distinguished [50]. The study of the flow-rate dependence in the glassy regime can probe the different timescales involved in the transition.

Acknowledgments—We acknowledge fruitful discussions with N. J. Wagner and O. D'Angelo. The authors gratefully acknowledge the scientific support and HPC resources provided by the German Aerospace Center (DLR). The HPC system CARO is partially funded by "Ministry of Science and Culture of Lower Saxony" and "Federal Ministry for Economic Affairs and Climate Action."

Data availability—The data that support the findings of this article are openly available [26].

[1] L. Tian and C. Bechinger, Surface melting of a colloidal glass, Nat. Commun. **13**, 6605 (2022).
[2] P. Zhang, J. J. Maldonis, Z. Liu, J. Schroers, and P. M. Voyles, Spatially heterogeneous dynamics in a metallic glass forming liquid imaged by electron correlation microscopy, Nat. Commun. **9**, 1129 (2018).
[3] S. F. Swallen, K. L. Kearns, M. K. Mapes, Y. S. Kim, R. J. McMahon, M. D. Ediger, T. Wu, L. Yu, and S. Satija, Organic glasses with exceptional thermodynamic and kinetic stability, Science **315**, 353 (2007).
[4] L. Berthier, P. Charbonneau, E. Flenner, and F. Zamponi, Origin of ultrastability in vapor-deposited glasses, Phys. Rev. Lett. **119**, 188002 (2017).
[5] C. Rodriguez-Tinoco, M. Gonzalez-Silveira, M. A. Ramos, and J. Rodriguez-Viejo, Ultrastable glasses: New perspectives for an old problem, Nuovo Cimento **45**, 325 (2022).
[6] M. D. Ediger and J. A. Forrest, Dynamics near free surfaces and the glass transition in thin polymer films: A view to the future, Macromolecules **47**, 471 (2014).
[7] H. Peng, H. Liu, and T. Voigtmann, Nonmonotonic dynamical correlations beneath the surface of glass-forming liquids, Phys. Rev. Lett. **129**, 215501 (2022).
[8] G. G. Fuller and J. Vermant, Complex fluid-fluid interfaces: Rheology and structure, Annu. Rev. Chem. Biomol. Eng. **3**, 519 (2012).
[9] N. O. Jaensson, P. D. Anderson, and J. Vermant, Computational interfacial rheology, J. Non-Newtonian Fluid Mech. **290**, 104507 (2021).
[10] H. Ragelle, M. W. Tibbitt, S.-Y. Wu, M. A. Castillo, G. Z. Cheng, S. P. Gangadharan, D. G. Anderson, M. J. Cima, and R. Langer, Surface tension-assisted additive manufacturing, Nat. Commun. **9**, 1184 (2018).
[11] C. Cammarota, A. Cavagna, G. Gradenigo, T. S. Grigera, and P. Verrocchio, Evidence for a spinodal limit of amorphous excitations in glassy systems, J. Stat. Mech. (2009) L12002.
[12] D. Ganapathi, K. H. Nagamanasa, A. K. Sood, and R. Ganapathy, Measurements of growing surface tension of amorphous-amorphous interfaces on approaching the colloidal glass transition, Nat. Commun. **9**, 397 (2018).
[13] T. Voigtmann, Nonlinear glassy rheology, Curr. Opin. Colloid Interface Sci. **19**, 549 (2014).
[14] *Theory and Applications of Colloidal Suspension Rheology* edited by N. J. Wagner and J. Mewis (Cambridge University Press, Cambridge, England, 2021).
[15] J. Boujlel and P. Coussot, Measuring the surface tension of yield stress fluids, Soft Matter **9**, 5898 (2013).
[16] L. Jørgensen, M. Le Merrer, H. Delanoë-Ayari, and C. Barentin, Yield stress and elasticity influence on surface tension measurements, Soft Matter **11**, 5111 (2015).
[17] W. Kob and H. C. Andersen, Testing mode-coupling theory for a supercooled binary Lennard-Jones mixture. II. Intermediate scattering function and dynamic susceptibility, Phys. Rev. E **52**, 4134 (1995).
[18] S. Plimpton, Fast parallel algorithms for short-range molecular dynamics, J. Comput. Phys. **117**, 1 (1995).
[19] G. Navascues, Liquid surfaces: Theory of surface tension, Rep. Prog. Phys. **42**, 1131 (1979).
[20] K. Birdi, *Surface Tension and Interfacial Tension of Liquids* (CRC, New York, 1997).
[21] P.-G. Gennes, F. Brochard-Wyart, D. Quéré *et al.*, *Capillarity and Wetting Phenomena: Drops, Bubbles, Pearls, Waves* (Springer, New York, 2004).
[22] M. Durand, Mechanical approach to surface tension and capillary phenomena, Am. J. Phys. **89**, 261 (2021).
[23] A. Marchand, J. H. Weijs, J. H. Snoeijer, and B. Andreotti, Why is surface tension a force parallel to the interface?, Am. J. Phys. **79**, 999 (2011).
[24] J. S. Rowlinson and B. Widom, *Molecular Theory of Capillarity* (Dover, New York, 1982).
[25] F. Varnik, J. Baschnagel, and K. Binder, Molecular dynamics results on the pressure tensor of polymer films, J. Chem. Phys. **113**, 4444 (2000).
[26] L. Heitmeier and T. Voigtmann, Lammps simulation script, Zenodo archive, 2025, https://zenodo.org/records/18444426.
[27] R. Evans, The nature of the liquid-vapour interface and other topics in the statistical mechanics of non-uniform, classical fluids, Adv. Phys. **28**, 143 (1979).

[28] S. W. Sides, G. S. Grest, and M.-D. Lacasse, Capillary waves at liquid-vapor interfaces: A molecular dynamics simulation, Phys. Rev. E **60**, 6708 (1999).
[29] R. Vink, J. Horbach, and K. Binder, Capillary waves in a colloid-polymer interface, J. Chem. Phys. **122** (2005).
[30] J. P. R. B. Walton, D. J. Tildesley, J. S. Rowlinson, and J. R. Henderson, The pressure tensor at the planar surface of a liquid, Mol. Phys. **48**, 1357 (1983).
[31] J. F. Lutsko and C. Schoonen, Classical density-functional theory applied to the solid state, Phys. Rev. E **102**, 062136 (2020).
[32] D. J Evans and G. P Morriss, *Statistical Mechanics of Nonequilbrium Liquids* (ANU Press, Canberra, Australia, 2007).
[33] A. H. Pelofsky, Surface tension-viscosity relation for liquids., J. Chem. Eng. Data **11**, 394 (1966).
[34] G. Di Nicola, M. Pierantozzi, S. Tomassetti, and G. Coccia, Surface tension calculation from liquid viscosity data of silanes, Fluid Phase Equilib. **463**, 11 (2018).
[35] G. Sun, S. Saw, I. Douglas, and P. Harrowell, Structural origin of enhanced dynamics at the surface of a glassy alloy, Phys. Rev. Lett. **119**, 245501 (2017).
[36] We use the "tensile" convention common in rheology, noting that some authors use a "compressive" convention with the opposite sign, noting $\sigma_{\alpha\alpha} = -p_\alpha$.
[37] U. M. B. Marconi, C. Maggi, and S. Melchionna, Pressure and surface tension of an active simple liquid: A comparison between kinetic, mechanical and free-energy based approaches, Soft Matter **12**, 5727 (2016).
[38] T. Speck, Stochastic thermodynamics for active matter, Europhys. Lett. **114**, 30006 (2016).
[39] J.-L. Barrat and L. Berthier, Fluctuation-dissipation relation in a sheared fluid, Phys. Rev. E **63**, 012503 (2000).
[40] J. M. Brader, T. Voigtmann, M. Fuchs, R. G. Larson, and M. E. Cates, Glass rheology: From mode-coupling theory to a dynamical yield criterion, Proc. Natl. Acad. Sci. U.S.A. **106**, 15186 (2009).
[41] C. F. Brooks, G. G. Fuller, C. W. Frank, and C. R. Robertson, An interfacial stress rheometer to study rheological transitions in monolayers at the air–water interface, Langmuir **15**, 2450 (1999).
[42] T. Verwijlen, P. Moldenaers, H. A. Stone, and J. Vermant, Study of the flow field in the magnetic rod interfacial stress rheometer, Langmuir **27**, 9345 (2011).
[43] N. Jaensson and J. Vermant, Tensiometry and rheology of complex interfaces, Curr. Opin. Colloid Interface Sci. **37**, 136 (2018).
[44] S. Naghieh and X. Chen, Printability—A key issue in extrusion-based bioprinting, Journal of pharmaceutical and biomedical analysis **11**, 564 (2021).
[45] S. Geisel, E. Secchi, and J. Vermant, Experimental challenges in determining the rheological properties of bacterial biofilms, Interface Focus **12**, 20220032 (2022).
[46] S. G. V. Charlton, A. N. Bible, E. Secchi, J. L. Morrell-Falvey, S. T. Retterer, T. P. Curtis, J. Chen, and S. Jana, Microstructural and rheological transitions in bacterial biofilms, Adv. Sci. **10**, 2207373 (2023).
[47] C. Clarke, F. Spyropoulos, and I. T. Norton, Surface rheological measurements of isolated food foam systems, Phys. Fluids **31**, 092002 (2019).
[48] C. Clarke, F. Spyropoulos, and I. T. Norton, A flow velocity dependence of dynamic surface tension in plateau borders of foam, J. Colloid Interface Sci. **573**, 348 (2020).
[49] N. Bain, A. Jagota, K. Smith-Mannschott, S. Heyden, R. W. Style, and E. R. Dufresne, Surface tension and the strain-dependent topography of soft solids, Phys. Rev. Lett. **127**, 208001 (2021).
[50] R. W. Style, A. Jagota, C.-Y. Hui, and E. R. Dufresne, Elastocapillarity: Surface tension and the mechanics of soft solids, Annu. Rev. Condens. Matter Phys. **8**, 99 (2017).